Carbonyl stretch of CH⋯O hydrogen-bonded methyl acetate in supercritical trifluoromethane

Maximiliano Inafuku, and Ernesto Marceca (iD)

View Online   Export Citation   CrossMark

ARTICLES YOU MAY BE INTERESTED IN

AIP Publishing

Carbonyl stretch of CH···O hydrogen-bonded methyl acetate in supercritical trifluoromethane

Maximiliano Inafuku and Ernesto Marceca[a] (ID)

AFFILIATIONS

Department of Inorganic, Analytical and Physical Chemistry-FCEN, University of Buenos Aires and INQUIMAE-CONICET, Ciudad Universitaria, Pab. II, Buenos Aires C1428EGA, Argentina

[a] Author to whom correspondence should be addressed: marceca@qi.fcen.uba.ar

ABSTRACT

Infrared spectroscopy in the gas phase was used to study the formation reaction of the CH···O hydrogen bonding complex involving the CH group of trifluoromethane, as a hydrogen donor, and the carbonyl group of methyl acetate, as a hydrogen acceptor, under different (T, p) conditions. The hydrogen-bonded carbonyl stretch of the molecular pair was monitored in dilute mixtures of methyl acetate in trifluoromethane at near-critical temperatures, from gas- to liquid-like densities. In the gas region, it was possible to discriminate the carbonyl signal of the hydrogen-bonded complex from that of the free ester and have access to their relative concentration. The equilibrium constant of the hydrogen bonding reaction and the standard enthalpy and entropy changes in the process were determined using the spectroscopic data. CH···O bonding was favored by lowering temperature or pressurizing F_3CH in the mixture, remaining essentially no free carbonyl groups about the critical density. The carbonyl band of the hydrogen-bonded pair appeared as a single symmetric peak up to liquid-like densities, suggesting that the 1:1 methyl acetate-trifluoromethane complex has the most abundant stoichiometry. Spectral features as frequency shift and bandwidth of the hydrogen-bonded carbonyl were studied as a function of temperature and solvent-density. A bathochromic (red) vibrational shift was registered for the bound carbonyl band against density, with a sudden change in behavior in the near-critical region, while the width of this band remains mostly unresponsive.

Published under license by AIP Publishing. https://doi.org/10.1063/5.0019058

I. INTRODUCTION

Hydrogen bonds are widespread among all kinds of materials and natural systems. They play an essential role in determining the structure at the molecular level of diverse chemical and biological structures, with consequences governing numerous physical, chemical, and life processes. Although most hydrogen bonds refer to XH···Y interactions, where X and Y are electronegative atoms (such as nitrogen, oxygen, or halogens), weaker CH···Y varieties involving the carbon atom as a hydrogen donor have also been described in the literature.[1–3] Despite their theoretically lower bond energies, such non-conventional hydrogen bonds are important in stabilizing different types of biomolecules[4] as well as complex supramolecular architectures.[5] CH···Y hydrogen bonds have been extensively characterized in solid systems,[6–8] even though they also take part in the hydrogen bonding structure of more disordered phases as

liquids.[9–12] New structural[12–14] and spectroscopic[13] aspects of the CH···O interaction in liquid mixtures were recently re-examined for the chloroform–acetone system, a well-known molecular model in which the CH moiety of chloroform behaves as a hydrogen donor and the acetone's carbonyl group as a hydrogen acceptor. The formation of $Cl_3CH···O=C(CH_3)_2$ complexes in solution is supported by various studies based on different techniques, principally those relying on IR and NMR spectroscopies.[3,9,15–17] However, since formation/rupture dynamics of such hydrogen bonding complexes occurs in the picosecond time scale,[18] NMR spectroscopy is inadequate to determine the concentration of each one of the interconverting structures. On the other hand, all the species involved in the hydrogen bonding equilibrium could in principle be quantified by IR light absorption, provided the bands can be discriminated in the spectrum. Bearing in mind that the vibrations more directly associated with a hydrogen bond (e.g., the XH···Y stretching

itself) have limited intensities and lie in the far-IR spectral region (<800 cm^{-1}),[19] the formation of complexes in the liquid is rarely corroborated by the appearance of a specific band in the spectrum. Instead, hydrogen bonding is more likely revealed by an energy shift in some of the bands of the complex,[8,20] or a change in the oscillator strength[21] of vibrations that are susceptible to the hydrogen interaction. For example, the interaction between chloroform and acetone has been studied in the liquid mixture by measuring the shift of the C=O fundamental frequency of acetone in the mid-IR spectrum.[17,22] Furthermore, red- or even blue-shifts in the CH vibration can also become truthful indicators that CH⋯Y complexes have been formed. This method has been applied to systems with a non-congested CH spectral region, for example, chloroform–acetonitrile and chloroform–ammonia, where the hydrogen bonding pairs were found to survive even in the gas phase at room temperature.[23,24]

From the point of view of quantum-chemical calculations, abundant information about CH⋯O/N molecular pairs is also available in the literature, most of which motivated in understanding why the CH vibration is occasionally blue-shifted when it is involved in a hydrogen bond.[11,25,26] The occurrence of red-, blue-, or no-shift in the CH vibrational mode was recently explained in terms of the electron density distribution along the CH⋯Y bond.[27]

While the use of vibrational probes to explore an interacting complex environment is widespread, the physics behind the observed spectral shifts or band broadening is still controversial and several theoretical approaches are available in the literature. For example, bathochromic solvent effects on the vibrational spectrum were traditionally attributed to dielectric stabilization of the dipolar probe inside a solvent cavity (reaction field),[28,29] changes in the probed frequency's force constant by coupling to the environment, and also energy shifts in the vibrational levels induced by the Stark interaction with the surrounding electric field.[30] In addition, a coarse but useful interpretation about the thermodynamic state dependence of vibrational shifts is given by the hard-sphere perturbation theory, in which the frequency change is related to the magnitude of attractive ($\Delta \nu_{max} < 0$) and repulsive ($\Delta \nu_{max} > 0$) components of the absorber–solvent interaction.[31,32]

The microsolvation environment of a molecule that is stabilized in a hydrogen bonding solvent by formation of hydrogen bridges will be in principle susceptible to the competition between solute–solvent and solvent–solvent hydrogen interactions. The possibility of adjusting the density by use of compressed supercritical fluids, in which phase separation does not occur, provides a means for fine tuning the degree of hydrogen bonding.[33–35]

In the present work, we studied the C=O stretch vibration of methyl acetate (MA) involved in a CH⋯O-type hydrogen bond with the CH group of trifluoromethane [or fluoroform (FL)] as a hydrogen donor. Solvent effects, as frequency shift and band shape changes in the C=O stretch signal, were investigated as a function of temperature and pressure, from gas- to liquid-like (dielectric constant: $\varepsilon \approx 6$) conditions, observing a peculiar behavior near the critical region of the fluid. At low density, a spectroscopic method was implemented to determine the concentration of the $F_3CH \cdots O=C(OCH_3)(CH_3)$ complex, giving us access to the equilibrium constant, enthalpy and entropy changes in the hydrogen bonding reaction between MA and FL.

II. EXPERIMENTAL

A. High-pressure IR spectrometry

Gaseous MA–FL mixtures at different pressures (1 bar–95 bars) and temperatures (294 K–373 K) were quantitatively examined by stationary infrared spectrometry. Spectral measurements were carried out using a cylindrical high-pressure optical cell installed in a FTIR apparatus with a nominal resolution of 1 cm^{-1} and averaging 128 scans. The spectral range of interest is 1700 cm^{-1} to 1900 cm^{-1}, which is located far enough from the strong absorption bands of the solvent (FL's CH stretch) that get saturated even at moderate densities. We monitored the C=O stretching band region (1710 cm^{-1} to 1815 cm^{-1}) comprising both free and hydrogen-bonded MA molecules,[36,37] and, additionally, we recorded the ($\nu_3 + \nu_5$) combination band of FL (1825 cm^{-1} to 1880 cm^{-1}) that is associated with the CF degenerate stretching (ν_5) and CF$_3$ symmetric deformation (ν_3).[38]

The optical cell was constructed in stainless steel, having calcium fluoride windows of 8 mm in diameter and 3.3 mm in thickness, which ensured a clean spectral window within 1500 cm^{-1} to 2500 cm^{-1}. The windows are sealed against the cell body by means of PCTFE o-rings, and the optical path length can be varied from 0.20 mm up to 4.35 mm, by using different fiber spacers. The cell's temperature, T, was maintained at the desired value within 0.3 K using an electric coil-formed heater powered by a proportional controller, and it was measured by means of a calibrated platinum thermometer. The cell is loaded through a stainless steel capillary that is connected to an ancillary gas handling system, consisting in a valved manifold with access to two built-in pressure transducers that can continuously monitor the cell's pressure, p, with an uncertainty of ±0.2 bar, for $p > 10$ bars, and ±0.1 bar, for $p < 10$ bars.

For each experimental run, a fresh MA–FL solution was prepared directly into the cell, by performing the following sequential operations in the valved manifold: (i) evacuate the cell and loading system, (ii) introduce gaseous MA into the cell by opening the valve of an external vessel containing liquid MA, (iii) isolate the cell and evacuate the loading system, (iv) open the cell's valve and slowly pressurize FL via a manual syringe pump until reaching the desired pressure, (v) maintain the cell connected to the pressure transducer and isolate from the loading manifold, and (vi) perform the spectroscopic measurement once the system reaches equilibrium. In the case of performing an isothermal run, in which increasing amounts of solvent are loaded into the cell, operations (iv)–(vi) must be repeated in each step. On the other hand, if one proceeds increasing T along an isobaric run, the system volume must be enlarged by controlling the position of a piston, in order to maintain the pressure at the desired value. The temperature of the vessel containing the solute, T_{MA}, was always maintained at least 5 K below the cell's temperature to avoid condensation of liquid on the optical windows. The molar density of MA in the cell, ρ_{MA}, can be adjusted through the vessel valve to a maximum value imposed by the vapor pressure of MA at T_{MA}.[39] More accurate ρ_{MA} values were determined by spectroscopic analysis.

B. Experimental runs

The carbonyl spectral region of low-density MA–FL mixtures was used to study the energetics of the $F_3CH \cdots O=C(OCH_3)(CH_3)$ hydrogen bonding process. We performed two isobaric runs at p = 2.0 ± 0.2 bars and 4.0 ± 0.2 bars (Tables SI-2 and SI-3, respectively), as a function of temperature, and one supercritical isotherm at T = 312.0 ± 0.3 K (Table SI-1) to a pressure of 6.8 bars. For these measurements, the optical path length of the cell was set to 4.35 mm. Two additional isothermal runs were performed at higher densities (Table SI-4), reaching pressures up to 95 bars: at 308.0 ± 0.3 K (supercritical) and at 294.0 ± 0.3 K (subcritical, liquid phase). In the high-density runs, the path length of the cell was reduced to 0.20 mm, avoiding the fact that the FL bands obscure the MA carbonyl signal. Typically, the molar density of MA in the mixture was maintained below a few tens of millimoles per liter (mM); that is, the solute mole fraction, x_{MA}, was kept below 0.15 for mixtures at moderate pressures ($p < 7$ bars), decreasing below 0.01 at higher pressures. On account of the high dilution at $p > 7$ bars, we assumed the fluid density equal to that of the pure solvent, at the same p and T, that is, $\rho = \rho_{MA} + \rho_{FL} \approx \rho_{FL}$, the latter being assessed using a fundamental equation of state for FL comprising the critical region.[40] At lower pressures, however, the assumption of considering x_{MA} negligible is no longer valid, and ρ must be determined using a spectroscopic method.

Dimensionless reduced variables were used to express the proximity to the critical region, defined as $T_r = T/T_{FL,c}$ and $\rho_r = \rho/\rho_{FL,c}$, where $T_{FL,c}$ = 299.29 K and $\rho_{FL,c}$ = 7.52 M refer to the critical point constants of pure FL. Anhydrous methyl acetate with 99.5% purity was purchased from Sigma-Aldrich, and trifluoromethane was from Matheson with 99.9% purity; both substances were transferred to the cell by distillation, without further purification.

C. Spectroscopic determination of the composition

The analytical method to determine the molar densities of the gaseous components of the mixture, namely, free (f) and hydrogen-bonded (HB) methyl acetate, as well as the solvent FL, relies on quantifying the baseline-subtracted absorption of representative peaks in the IR spectrum of the mixture, and also in the difference spectrum between the mixture and the pure solute. The measurement based on the peak integrated (area) or maximum absorbance (height) gave similar results (Fig. SI-1), although the second method is more easily implemented and robust. Hence, we chose to assess the molar density of the solvent by monitoring the maximum absorbance of a FL combination band located at $\nu \approx 1849$ cm^{-1}, A_ν, via the following relation:

$$\rho_{FL} = A_\nu/(b\,\varepsilon_{FL,\nu}), \tag{1}$$

where $\varepsilon_{FL,\nu}$ is the molar absorptivity and b represents the optical path length of the cell. The quantification of free and H-bonded solute molecules was done by analyzing the (partially resolved) two-peak carbonyl system. It was observed that the relative intensity between these two peaks visibly changes on going from pure MA to a mixture containing trifluoromethane, due to the formation of distinct H-bonded carbonyl absorbers. However, we will show that the high-energy peak of the carbonyl system is not affected by this

new absorption, and hence, a simple expression can be written, for the molar density of the free ester, as

$$\rho_f = A_{\nu''}/(b\,\varepsilon_{f,\nu''}), \tag{2}$$

where $A_{\nu''}$ stands for the high-energy peak absorbance at $\nu'' \approx 1777$ cm^{-1} and $\varepsilon_{f,\nu''}$ represents the molar absorptivity of free MA at ν''. As a corollary, the molar density of the H-bonded ester can be expressed as a function of the low-energy peak absorbance at $\nu' \approx 1760$ cm^{-1} of the solution, $A_{\nu'sl}$, and that of the pure solute, $A_{\nu'MA}$, according to

$$\rho_{HB} = (A_{\nu'sl} - A_{\nu'MA})/(b\,\varepsilon_{HB,\nu'}), \tag{3}$$

where ε_{HB} is the absorption coefficient of the H-bonded methyl acetate. Experimental access to ρ_{FL}, ρ_f, and ρ_{HB} in the mixture by use of Eqs. (1)–(3) requires the previous determination of the corresponding absorptivity coefficients. The absolute values of ε_{FL} and ε_f, corresponding to the two major components of the mixture, were numerically adjusted by fitting (to the experimental pressure) the pressure values calculated as

$$p = RT/(\bar{V} - B), \tag{4}$$

where $\bar{V} = (\rho_{FL} + \rho_f + \rho_{HB})^{-1}$ stands for the molar volume of the gaseous mixture and B is the second virial coefficient used to account for the non-ideality of the fluid. In this calculation, we used all the data points measured at pressures below 7 bars (Tables SI-1–SI-3), with the mean difference between the calculated and experimental pressure values being equal to 5%. Following this procedure led to the following results: $\varepsilon_{FL,1849}$ = 2.6 M^{-1} cm^{-1} and $\varepsilon_{f,1777}$ = 103.2 M^{-1} cm^{-1}. In addition, the ratio $\varepsilon_{HB}/\varepsilon_f$ was set equal to 3.2 and assumed temperature independent, based on previous quantitative IR measurements done for acetate carbonyl groups in miscible polymer blends[41] (see the supplementary material for further details).

III. RESULTS AND DISCUSSION

A. Thermodynamic study of the CH···O bond formation reaction

The fundamental C=O stretching band of pure MA in the gas phase IR spectra, at medium and high resolutions, exhibits discernible P and R rotational contours with no central Q branch features (B type), having absorption maxima at 1763 cm^{-1} and 1777 cm^{-1}.[36,42] *Ab initio* theoretical studies show that *cis*-MA is the most stable conformer, by 25 kJ mol^{-1} to 38 kJ mol^{-1}, with a rotational torsional barrier for the oxoester of 54 kJ mol^{-1},[43,44] which allows us to assign the measured IR spectrum exclusively to the *cis*-MA rotamer. As an example, the solid line in Fig. 1 exhibits the P–R structure associated with the C=O vibration of pure MA, in the gas phase, at 312.0 K (T_r = 1.04). When a small amount of gaseous FL was added into the cell, maintaining T invariant, the spectrum of the dilute mixture visibly changed. In particular, the low-energy peak evidenced a subtle red-shift, and its relative height was found to rise substantially as a function of the concentration of FL, as shown in Figs. 1(b)–1(d) (spectra are normalized by the high-energy peak).
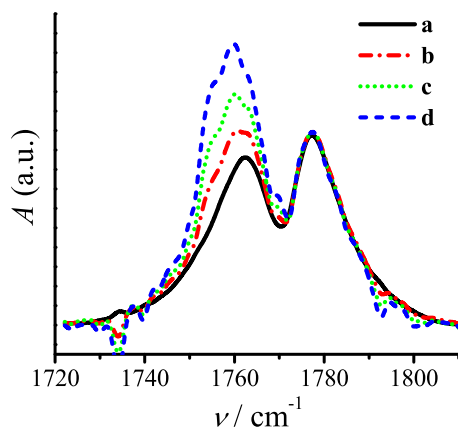
FIG. 1. Carbonyl stretching region of dilute ($x_{MA} < 0.04$) MA–FL mixtures, at T_r = 1.04 and low fluid densities: (a) pure gaseous MA; (b) ρ_r = 0.012 (p = 2.4 bars); (c) ρ_r = 0.023 (p = 4.4 bars); (d) ρ_r = 0.037 (p = 6.8 bars). For better comparison, spectra are normalized by the maximum absorption of the high-energy peak.

We have attributed the enhancement of the low-energy peak in MA–FL mixtures to the appearance of a new absorption band accounting for H-bonded carbonyl groups. Besides the notorious growth of this peak, shown in Fig. 1, an incipient non-resolved structure was also visualized at the peak maximum, which was absent in the spectrum of pure MA. Such spectral features in the low-energy peak become more evident at somewhat higher FL densities, which is consistent with a larger extent of hydrogen bonding and, hence, a more intense H-bonded carbonyl signal. The CH···O bond formation reaction can be written as

$$F_3CH + O=C(OCH_3)(CH_3) \rightleftharpoons F_3CH\cdots O=C(OCH_3)(CH_3). \quad (R1)$$
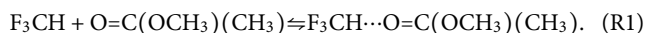
In contrast to the changes observed in the peak located at lower energy, the high-energy peak is practically unaltered by the presence of trifluoromethane, and this spectral characteristic was used to isolate the H-bonded carbonyl band component, as mentioned before. Decomposition of the overall absorption band into the non- and hydrogen-bonded components was attained by subtracting the (conveniently scaled) pure MA spectrum from that of the solution; that is, before subtraction, the spectrum of pure MA (recorded at the same temperature as the solution) must be scaled until matching the high-energy peak. The resulting free and bound MA components are shown in Fig. 2, for two experimental conditions. It is observed that, upon hydrogen bonding, the stretching frequency of H-bonded C=O shifts to lower wavenumbers with respect to the fundamental vibration of non-bonded C=O, located at the center of the P–R rotational structure of free MA (1770 cm^{-1}). This happens because the specific interaction between MA and FL withdraws electron density from the carbonyl group, and this weakens the strength of the C=O bond in the complex. The small red-shift in frequency measured for the C=O mode upon complexation at low pressure (-12 cm^{-1}) lies slightly under the *ab initio* values computed for the analogous Cl$_3$CH–acetone complex (-17 cm^{-1}),[13] F$_3$CH–O=CH$_2$ (-20 cm^{-1}),[25] and other H-bonded carbonyls with

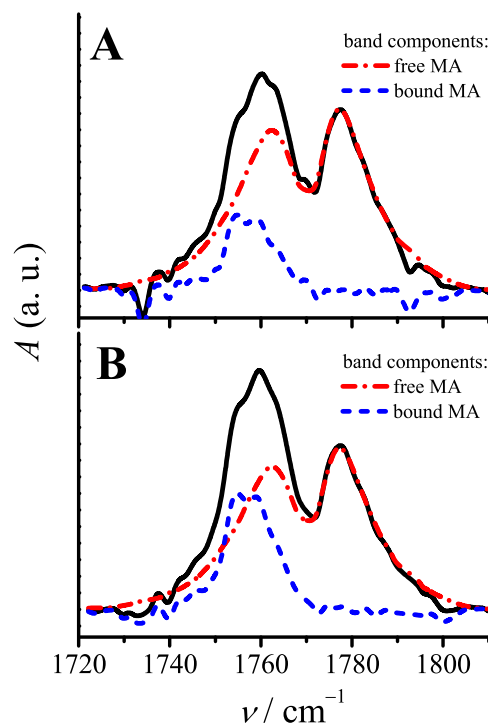**FIG. 2**. Carbonyl band system (solid line) for representative dilute ($x_{MA} < 0.04$) MA–FL mixtures, at T_r = 1.04. Free and H-bonded band components are shown. (A) ρ_r = 0.023 (p = 4.4 bars); (B) ρ_r = 0.037 (p = 6.8 bars). Spectra are normalized by the overall area.

HCl as a hydrogen donor (about -20 cm^{-1}).[45] Another characteristic of the carbonyl absorption is being narrower in the MA–FL H-bonded complex than in free MA, as expected for a structure with a larger moment of inertia, and it shows only an incipient rotational envelope, at our spectral resolution. As shown in Fig. 2, the proportion of bound/free carbonyl signals increases on going from panel (a) to (b) as a result of a higher FL density, which is clearly visualized as a relative enhancement of the low-energy peak.

Within the small density range of these experiments, we can easily use Eqs. (2) and (3) to evaluate the mole percent ratio of H-bonded carbonyls in the mixture, defined as %$_{HB}$ = 100 × $\rho_{HB}/(\rho_f + \rho_{HB})$. In Fig. 3, it is observed that at a constant temperature, this ratio increases steadily with density (larger concentration of FL in the mixture), reaching almost 16% at 312.0 K and a pressure of 6.8 bars [same conditions as in Fig. 2(B)]. Assuming the same (%$_{HB}$ vs ρ) variation to higher densities, one can estimate that at this temperature, %$_{HB}$ will reach 90% at a pressure of ~21 bars (ρ_r = 0.13). Moreover, it is also found that the extent of hydrogen bonding rapidly increases on lowering the temperature, along the isobaric runs, because of the exothermic character of the CH···O bond formation reaction.

In addition, Eqs. (1)–(3) allow us to determine the thermodynamic equilibrium constant of the association reaction (R1), in the gas phase, which is defined according to
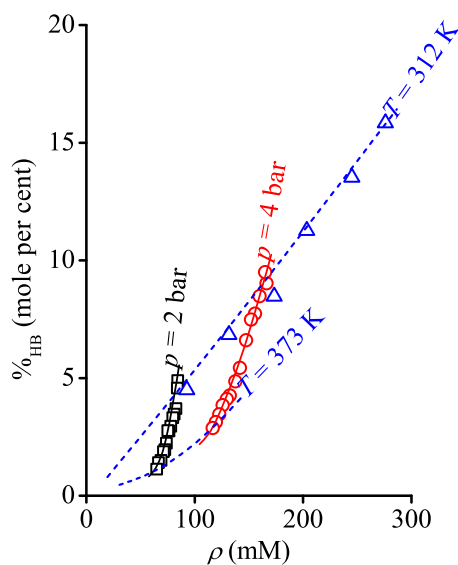
FIG. 3. Density dependence of the mole percent ratio of H-bonded carbonyls, $\%_{HB}$, in MA–FL mixtures ($x_{MA} < 0.13$), along an isotherm at $T = 312.0 \pm 0.3$ K ($T_r = 1.04$) and two isobars at $p = 2.0 \pm 0.2$ bars and 4.0 ± 0.2 bars, for $T > T_{FL,c}$.
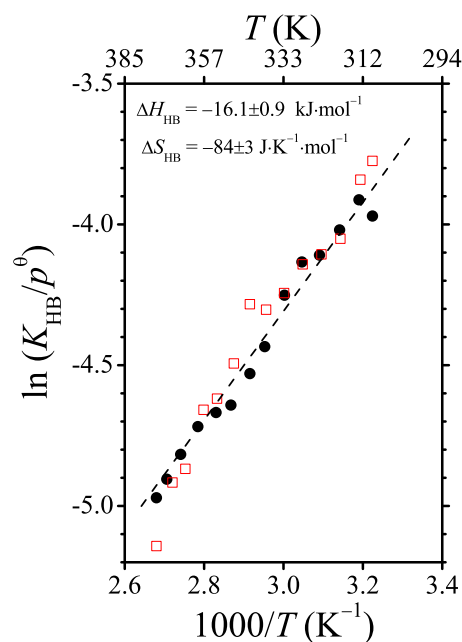

FIG. 4. van't Hoff plot on data points of isobar at $p = 4.0$ bars (black circles). Data points of isobar at $p = 2.0$ bars (red squares) are shown but not considered in the calculation. Enthalpy and entropy changes in the CH···O bond formation reaction (R1) were derived from a linear fit (slope = $-\Delta H_{HB}/R$; intercept = $\Delta S_{HB}/R$).

$$\frac{K_{HB}}{p^\theta} = \lim_{p \to 0} \frac{p_{HB}}{p_f \, p_{FL}}, \qquad (5)$$

where p_i represents the partial pressure of the i component in the mixture, and p^θ stands for the reference pressure (1 bar). For the isotherm at $T = 312$ K, a value of $K_{HB}/p^\theta = 0.018 \pm 0.002$ results by extrapolating the data points to $p \to 0$. This evidences that the CH···O bond in the complex F$_3$CH–MA is rather weak, as it is the case in other CH···X complexes like Cl$_3$CH–MA ($K_{HB}/p^\theta = 0.028$, $T = 323$ K)[46] or F$_3$CH–NH$_3$ ($K_{HB}/p^\theta = 0.024$, $T = 295$ K).[23]

The temperature dependence of the equilibrium constant of the CH···O bond formation reaction for the MA–FL system can be visualized in Fig. 4. Data points of the $p = 2.0$ bars (red squares) and $p = 4.0$ bars (black circles) isobars are plotted in the figure, although only the latter were considered in the van't Hoff fit due to their smaller dispersion. The values shown for the thermodynamic quantities ΔH_{HB} and ΔS_{HB} were determined from the slope and intercept of the linear fit, respectively. The measured value for the enthalpy change corresponds to a standard energy change of -13.5 kJ mol^{-1}, with the absolute value of this magnitude being almost identical to the computed binding energy for an akin intermolecular complex, such as F$_3$CH–acetone (13.9 kJ mol^{-1}),[11] and somewhat smaller than the values calculated for other FL complexes with stronger hydrogen acceptors, such as F$_3$CH–OH$_2$ (15.5 kJ mol^{-1})[25] and F$_3$CH–NH$_3$ (15.07 kJ mol^{-1}).[23] The binding energy involving the CH group of chloroform as a hydrogen donor is generally larger as, for example, in the Cl$_3$CH–acetone prototypic case, for which the informed calculated binding energy is within 17.9 kJ mol^{-1} to 16.4 kJ mol^{-1}.[11,13] Although weak, the exothermic hydrogen bonding energy is the driving force of reaction R1, counteracting the net entropy loss that occurred upon complexation ($\Delta S_{HB} = -84$ J K^{-1} mol^{-1}). The

complexation entropy of the MA–FL system lies above the values found in the literature for other H-bonded dimers with stronger hydrogen donors, for example, ClH–acetone (-91 J K^{-1} mol^{-1}),[47] or ClH- and FH- complexes with small aliphatic ethers (-80 to -120 J K^{-1} mol^{-1}).[48,49] The sign and magnitude of ΔS_{HB} reveal that the formation of a CH···O bond in the gas phase must overcome a large entropic barrier, which originates from the annihilation of translational and rotational degrees of freedom. Such negative entropy components dominate over the vibrational entropy gained just as the new CH···O bond is formed. The quantum chemical evaluation of ΔS_{HB} is often inaccurate due to the approximations used to calculate the low frequency modes that are inherent to these weak H-bonded complexes.[50,51]

The former experiments illustrate that, under such low-density conditions ($p < 4$ bars), the specific interaction in the MA–FL complex is minimally perturbed by surrounding solvent molecules, as inferred from the small pressure dependence of K_{HB} (see the supplementary material for further details). In addition, the linearity attained in the van't Hoff plot shown in Fig. 4 indicates that ΔH_{HB}, and hence the CH···O bond strength, does not change significantly with temperature, for T below 373 K.

B. Solvent effects on the H-bonded carbonyl band

When the density increases, the coupling of the H-bond molecular pair to the surrounding solvent is larger, and the CH···O bond strength is perturbed. However, considering that this bond is about two times stronger than the solvent–solvent CH···F bond,[52] the

H-bond integrity in the MA–FL complex will largely be conserved. At low density, solvent effects are usually rationalized in terms of the interaction between the MA–FL complex and the FL molecule, while in dense mixtures, they are more conveniently explained in terms of the macroscopic properties of the fluid, like the dielectric constant and its dependence on ρ_r. In this section, we show the density dependence found for the H-bonded carbonyl band shift and broadening.

At low density, we saw that free and H-bonded carbonyls have superimposed absorption bands, the latter being only assessed by subtracting the pure MA spectrum from that of the mixture (Fig. 2). However, when the FL density increases, the two-peak carbonyl system gradually changes into a unique peak, because of the consumption of free MA molecules by mass action [reaction (R1)] toward the formation of the complex. For reduced densities above ~0.25, no absorption is left at $\nu'' \approx 1777$ cm^{-1}, implying that under such conditions, it can be accepted that the spectrum is totally governed by the H-bonded MA–FL complex. In Fig. 5, we have plotted the density dependence of the bound carbonyl band, combining difference spectra (H-bonded components) measured at low densities with representative traces (single peaks) recorded within
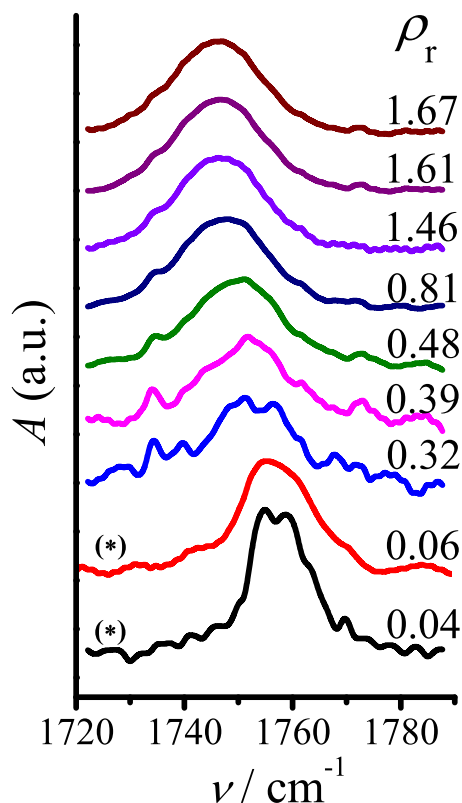
$\rho_r = 0.31–1.66$. The band is found to red-shift and broaden with increasing density.

Unlike the behavior of MA interacting with FL, where a unique signal persists in the IR spectra to liquid-like densities (e.g., $\rho_r = 1.67$ in Fig. 5), MA in water (D$_2$O) evidences two well resolved H-bonded carbonyl peaks ($\Delta\nu = 24$ cm^{-1}) attributed to the interconverting complexes: MA(D$_2$O)$_1$ and MA(D$_2$O)$_2$.[18,53] The presence of a single IR absorption in dense MA–FL mixtures is therefore a sign that the 1:2 complex is not formed in this system, making a difference between the behavior of OH$\cdots$O bonds and the weaker CH$\cdots$O bonds. Another reason against the formation of a 1:2 complex in dense MA–FL mixtures is that, with the F$_3$CH molecule having a single hydrogen donor site, the FL–FL interaction in the 1:2 complex is adverse.

The carbonyl band position, ν_{max}, is more clearly represented in Fig. 6 as a function of ρ_r, the latter being the best magnitude for analyzing the variation of fluid properties near the critical region. As it is usually found in supercritical mixtures,[54] three density regions are distinguished in the plot. Along the isotherm at $T_r = 1.03$, ν_{max} values drop quasi-linearly within a wide density range, up to $\rho_r = 0.6$. Next, the (ν_{max} vs ρ_r) slope changes drastically in the critical region ($\rho_r = 0.8–1.2$), where the spectral shift practically ceases, and, finally, a new change is observed at higher densities, where ν_{max} red-shifts again with a smaller slope than in the low-density region.

For $\rho_r < 0.6$, the observed density effect on ν_{max} could basically be attributed to short-range dipolar and H-bond interactions around the MA–FL complex, increasing in number as the inner solvation shell is built up. As the density increases, a growing frequency red-shift ($\Delta\nu_{max} < 0$) is indicative of a prevailing attractive complex–solvent interaction,[31,32] with a linear variation predicted,

FIG. 5. Spectral evolution of the H-bonded carbonyl band as a function of density for representative dilute ($x_{MA} < 0.04$) MA–FL mixtures, at $T_r = 1.03 \pm 0.01$. Low density peaks marked with (∗) result from the decomposition of the experimental band system (the H-bonded component is only shown). All the bands are normalized by area.
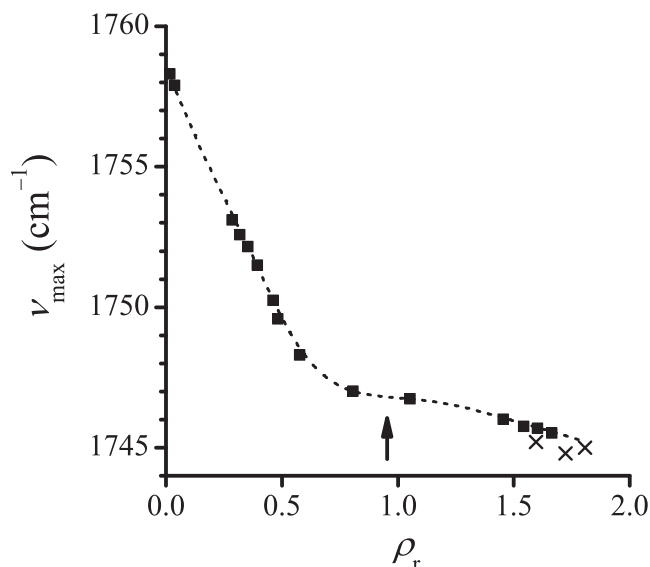

FIG. 6. Density dependence of the carbonyl maximum absorption frequency (ν_{max}) for dilute ($x_{MA} < 0.04$) MA–FL mixtures, at $T_r = 1.03$ (■) and 0.98 (×). Compressibility maximum at $T_r = 1.03$ is indicated by an arrow.

e.g., by a fully attractive model under a mean field approximation.[55] Such linear density-dependent red-shifts have also been reported for Raman and infrared C=O frequencies in other predominantly attractive systems, such as ketones and esters (including MA) dissolved in supercritical CO_2 ($T_r = 1.02$),[56] and also for metal carbonyls dissolved in supercritical ethane, CO_2, and FL.[57] The sudden change in trend observed in Fig. 6 at $\rho_r \approx 0.6$ probably happens when the first solvation shell of the MA–FL complex becomes saturated.

It is well established that near the gas–liquid critical state (about $\rho_r \approx 1$), the spectral behavior is not governed by solute–solvent interactions but by the critical phenomenon itself. The usual argument to support that the observable ν_{max} becomes unresponsive in this region is based on the existence of long-range density fluctuations at the microscopic level, i.e., dense solvent regions—specifically, those surrounding solute molecules—coexisting with extended fluid voids. Such highly compressible regions in the fluid are apparently able to minimize the effect of bulk density on the solvation micro-environment of the probe, and this makes the spectrum insensitive to ρ_r. A near-critical behavior of this kind was observed previously for many molecular probes and explained in terms of either local enhancement of solvent molecules around the solute (critical clustering or local density augmentation)[58] or the cancellation of rapidly changing quantities in the vicinity of the critical density.[57] In this case, we arrived at the same observation (i.e., a plateau in ν_{max}) for a CH···O H-bonded complex as a solute.

In the high-density region ($\rho_r > 1.4$), the abundance of fluid voids decreases significantly, and the spectroscopic properties become dependent on solute–solvent interactions again. In this density region, the C=O vibrational frequency of the MA–FL complex red-shifts once more vs ρ_r, but this time showing a weak slope, as a result of the smaller stabilization energy supplied by solvent molecules beyond the first solvent shell. A question arises whether the decrease in ν_{max} shown in the dense fluid can principally be attributed to the electrostatic stabilization of the H-bonded complex's dipole moment in the vibrational transition. Assuming that the MA–FL complex is immersed in a solvent continuum characterized by just a dielectric constant, ε (i.e., disregarding the existence of any complex–solvent specific interaction), the data in Fig. 6 should be well correlated with a measure of fluid's polarity. This effectively happens, in a broad view, observing larger red-shifts for increasing ε-values, according to a stronger stabilization of the C=O dipole. Moreover, the small temperature effect in the high-density region of Fig. 6, leading to an additional red-shift by decreasing T ($\Delta T = -14$ K), can also be ascribed to a higher fluid polarity by lowering the temperature (ε increases about 5% in this temperature range). However, it is only in a very limited density range that the spectroscopic evidence obeys the general prediction of classical theories, where the solvent reaction field is defined by dielectric continuum functions, $f(\varepsilon)$. For example, linear correlation between $\Delta\nu_{max}$ and Kirkwood's formula, $f(\varepsilon) = (\varepsilon - 1)/(2\varepsilon + 1)$, expected for a nonpolarizable dipolar oscillator in a continuous dielectric cavity,[28,29] is only valid in the liquid-like region, but rapidly fails at lower densities ($\rho_r < 1.2$). That is, $\Delta\nu_{max}$ data lie several wavenumbers below the classical prediction showing that, aside from the electrostatic (ε-dependent) effect, an additional specific density-dependent stabilization must be exerted on the C=O dipole (Fig. SI-2).

We turn next to analyze the second spectroscopic feature observed in the spectra of Fig. 5, concerning the density dependence of the C=O vibrational broadening. The bandwidth of the H-bonded carbonyl signal, expressed as FWHM (full width at half maximum), is shown in the upper panel of Fig. 7 as a function of ρ_r. Two density regions having different behavior can be distinguished. In the gas region, the C=O bandwidth increases rapidly with density, starting at ~12 cm^{-1} and reaching a 20 cm^{-1} plateau at a rather low density (below $\rho_{FL,c}/2$) and, next, the bandwidth remains practically invariant up to liquid-like densities, with no singular behavior near $\rho_r = 1$. With the carbonyl stretch being a well localized mode, such a step-like function in the measured FWHMs may simply reveal the early stages of the complex–solvent coupling. For $\rho_r > 0.4$, the C=O bandwidth remains unresponsive far beyond the critical region, denoting small configurational changes in the carbonyl group. For comparison, in the lower panel of Fig. 7, the (FWHM vs ρ_r) dependence corresponding to a combination band of neat FL (CF_3 deformation and CF stretching) is plotted, which, in view of the large excess of solvent molecules, only responds to FL–FL interactions. The strong broadening and weak tendency to abrupt saturation evidence, in this case, that multiple configurations coexist in the H-bonding network of FL molecules. Interestingly, although one expects a larger molecular disorder with increasing temperature, the opposite tendency was found in the H-bonded carbonyl FWHMs. This is probably a consequence of having a weaker complex–solvent interaction by
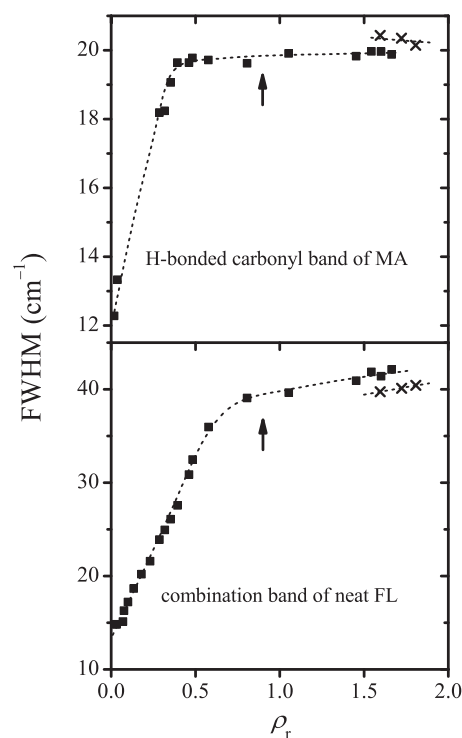

FIG. 7. Density dependence of selected spectral bandwidths (FWHM), at $T_r = 1.03$ (■) and 0.98 (×). Upper panel: H-bonded carbonyl band of MA for dilute ($x_{MA} < 0.04$) MA–FL mixtures; lower panel: combination band of neat FL (CF_3 deformation and CF stretching). Compressibility maximum at $T_r = 1.03$ is indicated by an arrow.

increasing T and, hence, a smaller frequency dispersion related to the H-bonded carbonyl vibration.

IV. CONCLUSIONS

In summary, we performed a gas-phase spectroscopic study of the hydrogen bonding reaction between the CH group of trifluoromethane as a hydrogen donor and the carbonyl group of methyl acetate as a hydrogen acceptor under different (T, p) conditions. Spectroscopic evidence supporting the formation of an H-bonded complex was found at near-critical temperatures, from gas- to liquid-like densities, with predominance of this species over free methyl acetate above the critical density. In the gas region, H-bonded C=O absorbs 11 cm^{-1} red-shifted from free C=O because electron charge is withdrawn from this group upon the formation of the CH···O bond. An additional red-shift of up to 12 cm^{-1} can gradually be exerted on the H-bonded carbonyl band by tuning the solvent-density up to $\rho_r \approx 1.7$, the shift only becoming unresponsive in the near-critical region. The spectroscopic evidence also points out that the methyl acetate–trifluoromethane complex has a 1:1 stoichiometry. Finally, thermodynamic analysis performed on the hydrogen bonding reaction allowed us to estimate an intermolecular binding energy of 13.5 kJ mol^{-1} for the MA–FL complex and a net entropy loss upon complexation of 84 J K^{-1} mol^{-1}.

SUPPLEMENTARY MATERIAL

See the supplementary material for tabulated results and further information about data treatment.

ACKNOWLEDGMENTS

DATA AVAILABILITY

The data that support the findings of this study are available within the article and its supplementary material.

REFERENCES

[1] G. R. Desiraju, Acc. Chem. Res. **24**, 290 (1991).

[2] P. Hobza and Z. Havlas, Chem. Rev. **100**, 4253 (2000).

[3] G. R. Desiraju and T. Steiner, *The Weak Hydrogen Bond* (Oxford University Press, 2001).

[4] O. O. Brovarets', Y. P. Yurenko, and D. M. Hovorun, J. Biomol. Struct. Dyn. **32**, 993 (2014).

[5] G. R. Desiraju, Acc. Chem. Res. **29**, 441 (1996).

[6] A. N. Campbell and E. M. Kartzmark, Can. J. Chem. **38**, 652 (1960).

[7] G. R. Desiraju, Acc. Chem. Res. **35**, 565 (2002).

[8] T. Steiner, Angew. Chem., Int. Ed. **41**, 48 (2002).

[9] S. Glasstone, Trans. Faraday Soc. **33**, 200 (1937).

[10] P. Jedlovszky and L. Turi, J. Phys. Chem. B **101**, 5429 (1997).

[11] S. N. Delanoye, W. A. Herrebout, and B. J. van der Veken, J. Am. Chem. Soc. **124**, 11854 (2002).

[12] J. J. Shephard, S. K. Callear, S. Imberti, J. S. O. O. Evans, and C. G. Salzmann, Phys. Chem. Chem. Phys. **18**, 19227 (2016).

[13] P. D. Vaz, M. M. Nolasco, F. P. S. C. Gil, P. J. A. Ribeiro-Claro, and J. Tomkinson, Chem. - Eur. J. **16**, 9010 (2010).

[14] S. Schreck, A. Pietzsch, B. Kennedy, C. Såthe, P. S. Miedema, S. Techert, V. N. Strocov, T. Schmitt, F. Hennies, J.-E. Rubensson, and A. Föhlisch, Sci. Rep. **7**, 20054 (2016).

[15] C. M. Huggins, G. C. Pimentel, and J. N. Shoolery, J. Chem. Phys. **23**, 1244 (1955).

[16] G. J. Korinek and W. G. Schneider, Can. J. Chem. **35**, 1157 (1957).

[17] K. B. Whetsel and R. E. Kagarise, Spectrochim. Acta **18**, 329 (1962).

[18] M. Candelaresi, M. Pagliai, M. Lima, and R. Righini, J. Phys. Chem. A **113**, 12783 (2009).

[19] D. J. Bakker, A. Dey, D. P. Tabor, Q. Ong, J. Mahé, M.-P. Gaigeot, E. L. Sibert, and A. M. Rijs, Phys. Chem. Chem. Phys. **19**, 20343 (2017).

[20] P. M. Kiefer, E. Pines, D. Pines, and J. T. Hynes, J. Phys. Chem. B **118**, 8330 (2014).

[21] A. V. Iogansen, Spectrochim. Acta, Part A **55**, 1585 (1999).

[22] M. R. Jalilian and L. Alibabaei, Spectrochim. Acta, Part A **62**, 322 (2005).

[23] M. Hippler, J. Chem. Phys. **127**, 084306 (2007).

[24] B. Behera and P. K. Das, J. Phys. Chem. A **123**, 1830 (2019).

[25] Y. Gu, T. Kar, and S. Scheiner, J. Am. Chem. Soc. **121**, 9411 (1999).

[26] I. V. Alabugin, M. Manoharan, S. Peabody, and F. Weinhold, J. Am. Chem. Soc. **125**, 5973 (2003).

[27] J. Joseph and E. D. Jemmis, J. Am. Chem. Soc. **129**, 4620 (2007).

[28] J. G. Kirkwood, J. Chem. Phys. **2**, 351 (1934).

[29] L. Onsager, J. Am. Chem. Soc. **58**, 1486 (1936).

[30] S. H. Schneider, H. T. Kratochvil, M. T. Zanni, and S. G. Boxer, J. Phys. Chem. B **121**, 2331 (2017).

[31] D. Ben-Amotz and D. R. Herschbach, J. Phys. Chem. **97**, 2295 (1993).

[32] X. Pan, J. Cooper McDonald, and R. A. MacPhail, J. Chem. Phys. **110**, 1677 (1999).

[33] M. Osada, K. Toyoshima, T. Mizutani, K. Minami, M. Watanabe, T. Adschiri, and K. Arai, J. Chem. Phys. **118**, 4573 (2003).

[34] S. Sala, Y. Danten, N. Ventosa, T. Tassaing, M. Besnard, and J. Veciana, J. Supercrit. Fluids **38**, 295 (2006).

[35] R. B. Gupta, C. G. Panayiotou, I. C. Sanchez, and K. P. Johnston, AIChE J. **38**, 1243 (1992).

[36] J. K. Wilmshurst, J. Mol. Spectrosc. **1**, 201 (1957).

[37] O. W. Kolling, J. Phys. Chem. **96**, 6217 (1992).

[38] H. D. Rix, J. Chem. Phys. **21**, 1077 (1953).

[39] J. Polák and I. Mertl, Collect. Czech. Chem. Commun. **30**, 3526 (1965).

[40] A. G. Aizpiri, A. Rey, J. Davila, R. G. Rubio, J. A. Zollweg, and W. B. Streett, J. Phys. Chem. **95**, 3351 (1991).

[41] E. J. Moskala, S. E. Howe, P. C. Painter, and M. M. Coleman, Macromolecules **17**, 1671 (1984).

[42] V. A. Walters, S. D. Colson, D. L. Snavely, K. B. Wiberg, and B. M. Jamison, J. Phys. Chem. **89**, 3857 (1985).

[43] K. B. Wiberg and K. E. Laidig, J. Am. Chem. Soc. **109**, 5935 (1987).

[44] K. Byun, Y. Mo, and J. Gao, J. Am. Chem. Soc. **123**, 3974 (2001).

[45] W. O. George, B. F. Jones, R. Lewis, and J. M. Price, Phys. Chem. Chem. Phys. **2**, 4910 (2000).

[46] J. D. Lambert, J. S. Clarke, J. F. Duke, C. L. Hicks, S. D. Lawrence, and D. M. Morris, Proc. R. Soc. London, Ser. A **249**, 414 (1959).

[47] H. D. Mettee, J. E. Del Bene, and S. I. Hauck, J. Phys. Chem. **86**, 5048 (1982).

[48] R. K. Thomas, Proc. R. Soc. London, Ser. A **322**, 137 (1971).

[49] G. Govil, A. D. H. Clague, and H. J. Bernstein, J. Chem. Phys. **49**, 2821 (1968).

[50] D. S. Dudis, J. B. Everhart, T. M. Branch, and S. S. Hunnicutt, J. Phys. Chem. **100**, 2083 (1996).

[51] A. S. Hansen, Z. Maroun, K. Mackeprang, B. N. Frandsen, and H. G. Kjaergaard, Phys. Chem. Chem. Phys. **18**, 23831 (2016).

[52] E. Kryachko and S. Scheiner, J. Phys. Chem. A **108**, 2527 (2004).

[53] A. C. Guerin, K. Riley, K. Rupnik, and D. G. Kuroda, J. Chem. Educ. **93**, 1124 (2016).

[54] Y.-P. Sun and C. E. Bunker, Ber. Bunsengesellschaft Phys. Chem. **99**, 976 (1995).

[55] K. S. Schweizer and D. Chandler, J. Chem. Phys. **76**, 2296 (1982).

[56] D. Kajiya, M. Imanishi, and K. Saitow, J. Phys. Chem. B **120**, 785 (2016).

[57] R. S. Urdahl, D. J. Myers, K. D. Rector, P. H. Davis, B. J. Cherayil, and M. D. Fayer, J. Chem. Phys. **107**, 3747 (1997).

[58] S. A. Egorov and J. L. Skinner, J. Phys. Chem. A **104**, 483 (2000).